Connection Science
Publication details, including instructions for authors and subscription information:
http://www.informaworld.com/smpp/title~content=t713411269

Neural Nets with Markers and Gaussian-distributed Connectivities

E. Fournou[a]; P. Argyrakis[a]; P. A. Anninos[a]
[a] Department of Physics 313-1, University of Thessaloniki, Thessaloniki, Greece

To cite this Article Fournou, E. , Argyrakis, P. and Anninos, P. A.(1993) 'Neural Nets with Markers and Gaussian-distributed Connectivities', Connection Science, 5: 1, 77 — 94
To link to this Article: DOI: 10.1080/09540099308915686
URL: http://dx.doi.org/10.1080/09540099308915686

Neural Nets with Markers and Gaussian-distributed Connectivities

E. FOURNOU, P. ARGYRAKIS & P. A. ANNINOS

(Received for publication 2 June 1992; revised paper accepted 20 July 1992)

We investigate probabilistic neural nets with the inclusion of chemical markers and Gaussian distribution of the connectivities of the constituent neurons. We start from the studied case of Poisson distributions and extend it to an analogous formalism for the activity of a netlet with Gaussian characteristics. The analytical formulae are somewhat more complicated due to the presence of markers. The results show that the change from a Poisson to a Gaussian distribution may cause a net to change class if it belongs to class A, making it class B. This trend is similar to the one observed in the absence of markers. We also observe interesting trends in the variation of the sizes of the markers by isolating the contribution of each subnet to the overall activity. Finally, the general repercussions of the present work to our understanding of the dynamics of the brain network are discussed.

KEYWORDS: Neural modeling, chemical markers.

1. Introduction

Phylogenesis of the central nervous system from amphibia to mammals has been marked by the appearance of new brain structures as well as structural modifications and specialization of archaic structures. The emergence in mammals of a neocortex characterized by a multi-layered nerve cell arrangement, combined with the retention in the hippocampus of essentially monolayered paleocortex, constitutes an outstanding example of this evolutionary process. More detailed scrutiny reveals additional structural specializations; thus, sensory neocortex is five-layered, whereas the motor cortex shows much less distinct stratification. On the other hand, thalamic nuclei, with the exception of the lateral geniculate, do not show any clear laminar organization. The question naturally arises whether these structural features may reflect, and perhaps determine, fundamental differences in the mode of operation of distinct brain structures. Alternatively, the possibility may exist that such structural specializations merely represent anatomical 'accidents of development', perhaps reflecting phylogenetic origins, but playing a functional role

E. Fournou* & P. Argyrakis, Department of Physics 313-1, University of Thessaloniki, 54006 Thessaloniki, Greece. E-mail: cacz11@grtheun1. *Permanent address Department of Applied Sciences, Technological Education Institution (TEI) of Thessaloniki, 574 00 Sindos, Greece. P. A. Anninos, Department of Medical Physics, University of Thraki, 68100 Alexandroupolis, Greece.

no more significant than, for example, the appendix or the coccygeal vertebrae in man.

It is difficult to provide an answer to this question from the anatomical and physiological data currently available. Although substantial neurohistological and neurophysiological information is available, meaningful correlation of these two sets of data can only be accomplished in very isolated instances. In general, unlike recording from invertebrates, where the simplicity and viability of the nervous system make it feasible to observe the elements recorded from, physiological studies of the mammalian central nervous system (CNS) are performed in a 'blind' fashion and it is exceedingly difficult to correlate these studies with the microscopical anatomy of the tissue.

While the ultimate answer to the question of functional meaning of anatomical structure eventually must come from increased sophistication in experimental design and methodology, some insight may be obtained through the use of models. It is, of course, impossible to create a model which is a perfect replica of the system under study; to do so would presuppose perfect knowledge of the system, obviating the need for the model. Rather, one may choose a certain smaller subset of properties and employ the model to study the effect of these properties on the operation of the model.

In the present study, we investigate the relationship between structure, as expressed in patterns of interneuronal synaptic connectivity, and 'spontaneous' activity in finite nerve–cell assemblies. In constructing models of such neuron assemblies, connectivity among individual elements may be specified to follow a given probability law, maintaining all other parameters constant. It will be shown that the probability law selected to specify the connectivity pattern has a profound effect on subsequent activity in the system.

2. The Mathematical Formalism of the Model

The mathematical formalism is based on the same assumptions as in previous work (Harth *et al.*, 1970; Anninos *et al.*, 1970; Anninos & Elul, 1974; Anninos & Kokkinidis, 1984). The present model focuses on two points: the concept of chemical markers and the effect of the Gaussian pattern of interneuronal connectivity on the network activity. The past studies have assumed a Poisson pattern of interneuronal connectivity. Thus, we will present as a starting point the basic equations for the activity of an isolated netlet with N markers for the Poisson pattern and then we will derive the equations for the Gaussian case.

Neural nets are assumed to be constructed of discrete sets of randomly interconnected neurons of similar structure and function, termed *netlets*, but neural connections are set up by means of chemical markers carried by the individual cells, according to the theory of neural specificity (Sperry, 1943, 1963; Prestige & Willshaw, 1975). According to this theory, each neuron makes active synaptic connections only with those neurons in the network which carry markers with the highest chemical affinity to its own. Thus, the whole network is divided into neural subpopulations, each being characterized by its own marker. In a netlet with A neurons, each neuron at some instance may carry an electrical potential of a few millivolts, which it passes on to the neurons that it is connected to. The neuron is the elementary unit in these models, and it is a bistable element. It can be either in a resting or in an active (firing) state. The transition from the resting to the firing state of the neuron occurs when the sum of *postsynaptic potentials* (PSPs)

arriving at the cell exceeds a certain critical value, the threshold θ of the neuron. PSPs may be either excitatory (EPSPs) or inhibitory (IPSPs), shifting the membrane potential closer to or further away from θ, respectively. A fraction h ($0 < h < 1$) of a certain number of neurons out of the total may be inhibitory with all of their axon branches generating IPSPs, while the rest of the neurons will be excitatory with all of their axon branches generating EPSPs. A neuron receives, on average, μ^+ EPSPs and μ^- IPSPs. The size of the PSP produced by an excitatory (inhibitory) unit is $K^+(K^-)$.

If a neuron fires at time t, it produces the appropriate PSPs after a fixed time interval τ, the *synaptic delay*. PSPs arriving at a neuron are summed instantly, and if this sum exceeds θ, it will cause the neuron to fire immediately. Firing is momentary and causes the neuron to be insensitive to further stimulation for a time interval called the *refractory period*. PSPs, if below θ, will persist with or without decrement for a period of time called the *summation time*, which is assumed to be less than the synaptic delay. It is also assumed here that the refractory period is greater than the synaptic delay, but less than twice the synaptic delay. If a number of neurons fire simultaneously at time t, then all neural activity resulting from this initial activity will be restricted to times $t + \tau, t + 2\tau, \ldots$.

The dynamic variable that is monitored here is the level of activity a_n, i.e. the fraction of neurons in the netlet that are active at $t = n\tau$. This quantity is a scalar and does not specify which particular neurons are firing in the netlet. The activity a_n at time $t = n\tau$ depends exclusively on the firing record of the netlet at time $t = (n-1)\tau$. Therefore, the dynamics of the netlet is a Markov process. The expectation value $< a_{n+1} >$ of the activity at time $t = (n+1)\tau$, is the average value of a_{n+1} generated by a collection of netlets with identical structural parameters and the same a_n. It is also assumed that all subsystems in the netlet with different markers are assigned the same fraction of active neurons a_n. The important constraint of markers gives rise to ordered patterns of nerve connections. Notwithstanding, the interconnections between the neurons are assumed to be made up at random; active connections are considered to be only these that belong to cells which carry the same type of marker. To be more specific, neural connections exist at random with no restriction among all cells, just as in the case with no markers, but the EPSPs (and IPSPs) are carried only to the connections that belong to the same marker. Connections between neurons of different markers are inactive, i.e. they carry no signal. The total number of the A neurons is therefore divided into several such subpopulations. If $m_1, m_2, \ldots, m_N$ are the fractions of neurons in a network of N markers corresponding to each subpopulation, then obviously, $m_1 + m_2 + \cdots + m_N = 1$.

2.1. *Poisson Distribution*

The quantity $< a_{n+1} >$ is calculated similarly to previous studies (Harth *et al.*, 1970; Anninos *et al.*, 1970). In a netlet with A neurons and N markers, if a_n is the activity at time $t = n\tau$ and m_j, h_j ($j = 1, 2, \ldots, N$) are the fraction of neurons and the fraction of inhibitory neurons, respectively, carrying the jth marker in the netlet, then the expectation value of the activity in the netlet at time $t = (n+1)\tau$, for the Poisson approximation, is given by (Anninos & Kokkinidis, 1984):

$$< a_{n+1} > = (1 - a_n) \sum_{j=1}^{N} m_j \sum_{I=0}^{I_{\max,j}} (1 - \sum_{L=0}^{\eta'_j - 1} P_{L,j}) Q_{I,j} \tag{1}$$

This equation results by adding all probabilities for all combinations of thresholds and PSPs that produce firing. The quantity

$$P_j(a_n, m_j, \theta_j) = \sum_{I=0}^{I_{\max,j}} (1 - \sum_{L=0}^{\eta'_j - 1} P_{L,j}) Q_{I,j} \tag{2}$$

is the probability that a neuron of the jth marker receives a PSP which exceeds its threshold θ_j, and is expressed here in terms of Poisson distributions of the number of excitatory and inhibitory inputs to a cell. $P_{L,j}$ and $Q_{I,j}$ are the probabilities that a neuron of the jth marker will receive L-EPSPs and I-IPSPs at time $t = (n + 1)\tau$, and they are given by

$$P_{L,j} = \exp[-a_n \mu_j^+ (1 - h_j) m_j] [a_n \mu_j^+ (1 - h_j) m_j]^L / L! \tag{3}$$

and

$$Q_{I,j} = \exp(-a_n \mu_j^- h_j m_j) (a_n \mu_j^- h_j m_j)^I / I! \tag{4}$$

The upper limit $I_{\max,j}$ in the sum is the total number of active inhibitory connections of the netlet in the subsystem of the jth marker, and is given by

$$I_{\max,j} = A a_n \mu_j^- h_j m_j \tag{5}$$

while η'_j in the upper limit in the inner sum is the minimum number of excitatory inputs necessary to trigger a neuron which has received I inhibitory inputs and carries marker j. It is given by

$$\eta'_j = u[\theta_j + I K_j^-) / K_j^+] \tag{6}$$

The function $u[x]$ is defined as the smallest integer which is equal to or greater than x.

The behavior at the origin of equation (1) is also of interest in this treatment. Thus we must take an expression for the slope of the curve $< a_{n+1} >$ vs a_n as $a_n \to 0$, i.e. we must take $\partial / \partial a_n < a_{n+1} > | a_n = 0$, from equation (1). The result is

$$\frac{\partial}{\partial a_n} < a_{n+1} > |_{a_n = 0} = \begin{cases} \sum_{j=1}^{N} m_j^2 \mu_j^+ (1 - h_j) & \text{for every } \eta_j = 1 \\ 0 & \text{for every } \eta_j \geq 2 \end{cases} \tag{7}$$

where the parameter η_j is defined as the minimum number of EPSP necessary to trigger a neuron in the absence of inhibitory inputs, and it is given by $\eta_j = u[\theta_j / K_j^+]$.

2.2. Gaussian Distribution

Following the assumptions of previous papers (Anninos *et al.*, 1970; Anninos & Kokkinidis, 1984), we at first examine the case of an isolated netlet with two markers, a and b. We assume here (Anninos & Elul, 1974) that the number of input PSPs per neuron will follow a Gaussian distribution if the average number of active inputs per neuron becomes sufficiently large, according to de Moivre's approximation.

In a netlet of A neurons with two markers a and b, let m_a and $m_b = 1 - m_a$ be the fractions of neurons characterized with the chemical markers a and b, respectively, and h_a and h_b be the fractions of inhibitory neurons for the two markers, respectively. Let also $a_n A$ be the active neurons in the netlet at time $t = n\tau$. Then, one synaptic delay later, i.e. at $t = (n + 1)\tau$, a number $A a_n \mu_a^+ + (1 - h_a) m_a$ of

EPSPs and a number $Aa_n\mu_a^- h_a m_a$ of IPSPs will appear in the subnet of the a marker. Similarly, a number $Aa_n\mu_b^+(1-h_b)m_b$ of EPSPs and a number $Aa_n\mu_b^- h_b m_b$ of IPSPs will appear in the subnet of the b marker. On average, a number $\bar{l}_a = a_n\mu_a^+(1-h_a)m_a$ of EPSPs per neuron and a number of $\bar{i}_a = a_n\mu_a^- h_a m_a$ of IPSPs per neuron will appear in the subnet of the a marker, and similarly a number $\bar{l}_b = a_n\mu_b^+(1-h_b)m_b$ of EPSPs per neuron and a number $\bar{i}_b = a_n\mu_b^- h_b m_b$ of IPSPs per neuron will appear in the subnet of the b marker. If $l_a(l_b)$ is the number of EPSPs input to a given neuron of the $a(b)$ marker and $i_a(i_b)$ is the corresponding number of IPSPs, then the total PSP input to a neuron of the $a(b)$ marker, at time $t = (n+1)\tau$, is given by

$$e_{a,n+1} = l_a K^+ + i_a K^- \tag{8}$$

for marker a, and

$$e_{b,n+1} = l_b K^+ + i_b K^- \tag{9}$$

for marker b.

If all the quantities l_a, l_b, i_a and i_b are sufficiently large, their distributions may be approximated by normal distributions about their average values $\bar{l}_a$, $\bar{l}_b$, $\bar{i}_a$ and $\bar{i}_b$. Therefore, Gaussian distributors will also be the distributions of $e_{a,n+1}$ and $e_{b,n+1}$, since their variancies, $\delta^2_{a,n+1}$ and $\delta^2_{b,n+1}$, respectively, are sums of the corresponding variancies of l_a, i_a and l_b, i_b, and the probabilities for l_a, i_a, l_b and i_b are independent of one another. Thus, the mean PSP for the two markers a and b will be given by

$$\bar{e}_{a,n+1} = \bar{l}_a K^+ + \bar{i}_a K^- = a_n m_a[\mu_a^+(1-h_a)K^+ + \mu_a^- h_a K^-] \tag{10}$$

and

$$\bar{e}_{b,n+1} = \bar{l}_b K^+ + \bar{i}_b K^- = a_n m_b[\mu_b^+(1-h_b)K^+ + \mu_b^- h_b K^-] \tag{11}$$

and their vacancies by

$$\delta^2_{a,n+1} = a_n m_a[\mu_a^+(1-h_a)(K^+)^2 + \mu_a^- h_a(K^-)^2] \tag{12}$$

and

$$\delta^2_{b,n+1} = a_n m_b[\mu_b^+(1-h_b)(K^+)^2 + \mu_b^- h_b(K^-)^2] \tag{13}$$

respectively.

The probability $P_a(a_n, m_a, \theta_a)$ that the PSP exceeds a threshold θ_a for the a marker is now

$$P_a(a_n, m_a, \theta_a) = \frac{1}{\sqrt{(2\pi)}} \int_{x_{a,n+1}}^{\infty} e^{-x^2/2} dx \tag{14}$$

where

$$x_{a,n+1} = \frac{\theta_a - \bar{e}_{a,n+1}}{\delta_{a,n+1}} \tag{15}$$

and similarly, the probability $P_b(a_n, m_b, \theta_b)$ that the PSP exceeds a theshold θ_b for the b marker is

$$P_b(a_n, m_b, \theta_b) = \frac{1}{\sqrt{(2\pi)}} \int_{x_{b,n+1}}^{\infty} e^{-x^2/2} dx \tag{16}$$

where

$$x_{b,n+1} = \frac{\theta_b - \bar{e}_{b,n+1}}{\delta_{b,n+1}} \tag{17}$$

Since, as in other previous work (Anninos *et al.*, 1970; Anninos & Kokkinidis, 1984), we also assume here that all neurons that are active at $t = n\tau$ will be inactive at the next time step $t = (n + 1)\tau$, because of refractoriness, there are exactly $Am_a(1 - a_n)$ neurons in the a marker and $Am_b(1 - a_n) = A(1 - m_a)(1 - a_n)$ neurons in the b marker that are not in a refractory state at $t = (n + 1)\tau$. The expectation value of activity is therefore given by

$$< a_{n+1} > = (1 - a_n)[m_a P_a(a_n, m_a, \theta_a) + (1 - m_a)P_b(a_n, m_b, \theta_b)] \tag{18}$$

We may now proceed to a straightforward generalization for an isolated netlet of N chemical markers $m_1, m_2, m_3, \ldots, m_N$, where m_j is the fraction of neurons characterized by the jth chemical marker, and

$$m_1 + m_2 + m_3 + \ldots + m_N = \sum_{j=1}^{N} m_j = 1 \tag{19}$$

In analogy to equation (18), we may now write the following expression for the expectation value of the activity

$$< a_{n+1} > = (1 - a_n)\sum_{j=1}^{N} m_j P_j(a_n, m_j, \theta_j) \tag{20}$$

where $P_j(a_n, m_j, \theta_j)$ is the probability that a neuron of the jth marker receives a PSP which exceeds its threshold θ_j, and is given by the equation

$$P_j(a_n, m_j, \theta_j) = \frac{1}{\sqrt{(2\pi)}} \int_{x_{j,n+1}}^{\infty} e^{-x^2/2} dx \tag{21}$$

where

$$x_{j,n+1} = \frac{\theta_j - \bar{e}_{j,n+1}}{\delta_{j,n+1}} \tag{22}$$

$$\bar{e}_{j,n+1} = a_n m_j[\mu_j^+ (1 - h_j)K^+ + \mu_j^- h_j K^-] \tag{23}$$

and

$$\delta^2_{j,n+1} = a_n m_j[\mu_j^+ (1 - h_j)(K^+)^2 + \mu_j^- h_j (K^-)^2] \tag{24}$$

It is also of interest in this analysis to study the behavior of equation (20) at the origin, i.e. to find the slope of the curve $< a_{n+1} >$ vs a_n as $a_n \to 0$, in order to see the significance of the replacement of the Poisson probability distribution by a normal one, for the case of netlets with chemical markers. For this purpose, we first write equation (20) in the form

$$f(x_1, x_2, \ldots, x_N) = (1 - a_n)\sum_{j=1}^{N} m_j P_j(x_j) \tag{25}$$

where

$$x_j = \frac{\theta_j - \bar{e}_j}{\delta_j} \tag{26}$$

and then calculate the partial derivative of f with respect of a_n at $a_n \to 0$, i.e.

$$\frac{\partial f}{\partial a_n}\Big|_{a_n = 0} = \frac{\partial}{\partial a_n}[(1 - a_n)\sum_{j=1}^{N} m_j P_j(x_j)]\Big|_{a_n = 0} \tag{27}$$

from which we have

$$\frac{\partial f}{\partial a_n}\Big|_{a_n=0} = \left\{ -\sum_{j=1}^{N} m_j P_j(x_j) + (1-a_n)\sum_{j=1}^{N} m_j \frac{\partial P_j(x_j)}{\partial x_j}\frac{dx_j}{da_n}\right\}\Big|_{a_n=0} \tag{28}$$

Using equation (21) and applying Leibnitz's theorem we get

$$\frac{\partial P_j(x_j)}{\partial x_j} = -\frac{1}{\sqrt{(2\pi)}}\, e^{-x_j^2/2} \tag{29}$$

Taking $|K^+| = |K^-| = K$, $(0 < K < \infty)$ and $\eta_j = \theta_j/K^+$ it follows from equation (26) that

$$x_j = \frac{\eta_j - a_n[m_j\mu_j^+(1-h_j) + m_j\mu_j^- h_j]}{\sqrt{[a_n[m_j\mu_j^+(1-h_j) + m_j\mu_j^- h_j]]}} \tag{30}$$

Using $q_j = m_j\mu_j^+(1-h_j)$ and $p_j = m_j\mu_j^- h_j$ we get

$$x_j = \frac{\eta_j + a_n(p_j - q_j)}{\sqrt{[a_n(p_j + q_j)]}} \tag{31}$$

Differentiating this equation with respect to a_n we obtain

$$\frac{dx_j}{da_n} = \frac{-\eta_j^+ a_n(p_j - q_j)}{2a_n\sqrt{[a_n(p_j^+ q_j)]}} \tag{32}$$

Taking into account equations (29) and (32), equation (28) can be written in the form

$$\frac{\partial f}{\partial a_n}\Big|_{a_n=0} = \left\{ -\sum_{j=0}^{N} m_j P_j(x_j) - \frac{1-a_n}{\sqrt{(2\pi)}}\sum_{j=1}^{N} m_j e^{-x_j^2/2}\frac{-\eta_j + a_n(p_j - q_j)}{2a_n\sqrt{[a_n(p_j + q_j)]}}\right\}\Big|_{a_n=0} \tag{33}$$

from which, after some algebraic manipulation, we get

$$\frac{\partial f}{\partial a_n}\Big|_{a_n=0} = \left\{ -\sum_{j=0}^{N} m_j P_j(x_j) - \frac{1-a_n}{\sqrt{(2\pi)}}\sum_{j=0}^{N} m_j x_j e^{-x_j^2/2} + \frac{1-a_n}{a_n\sqrt{(2\pi)}}\sum_{j=1}^{N}\frac{m_j\eta_j}{\sqrt{[a_n(p_j+q_j)]}}\, e^{-x_j^2/2}\right\}\Big|_{a_n=0} \tag{34}$$

Since as $a_n \to 0$ the $x_j \to \infty$, then it can be easily seen by l'Hôpital's rule that

$$\lim_{a_n\to 0}\frac{\partial f(x_j)}{\partial a_n} \to 0 \tag{35}$$

3. Results

On the basis of equations (1) for the Poisson approximation of interconnectivity and equation (18) or (20) for the Gaussian one, we obtained plots of the expectation value of the activity $< a_{n+1} >$ as a function of the preceding activity a_n, for a wide variety of different combinations of parameters. We at first examined the effect of connectivity on dynamical behavior of isolated networks first with one and then with two markers, a and b. For six such networks with $m_a = 1.0$, 0.9, 0.8, 0.7, 0.6 and 0.5 for the a marker, and $m_b = 0.0$, 0.1, 0.2, 0.3, 0.4 and 0.5 for the b marker, respectively, we received the curves of $< a_{n+1} >$ vs a_n. These are shown in Figures 1 and 2. Solid lines are obtained by the Poisson approximation of the interneural connectivity while dashed lines by the Gaussian one. The curves in Figure 1(a) represent the total network activity for each of the above-mentioned

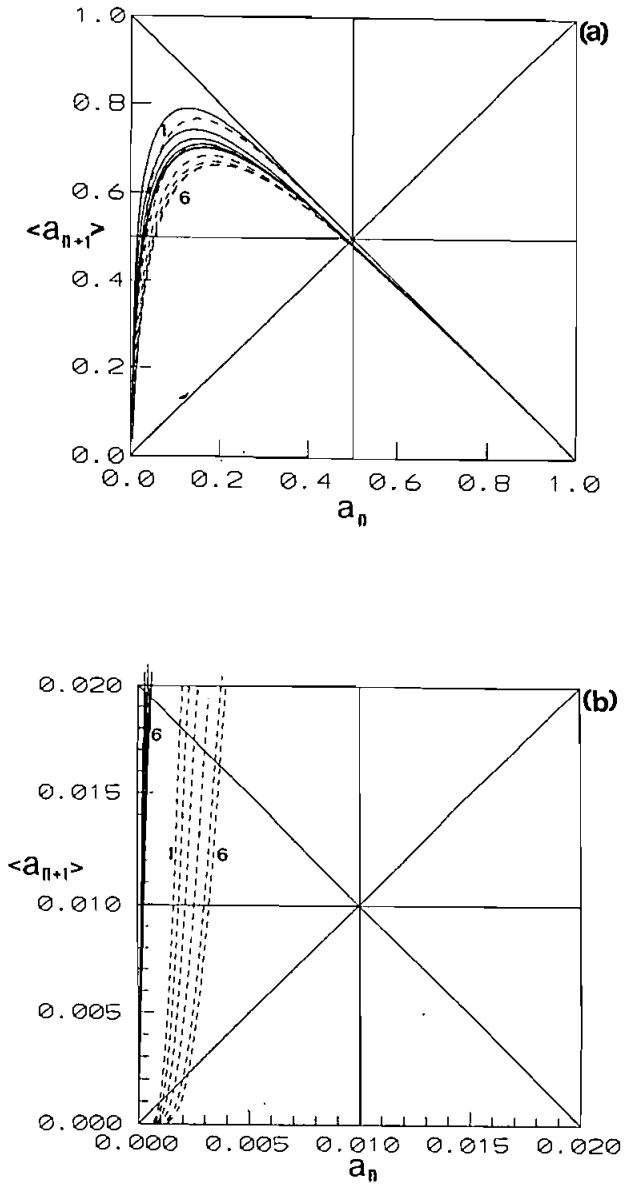

Figure 1. (a) Expectation value of the total neural activity $< a_{n+1} >$ vs preceding activity a_n for isolated netlets with two chemical markers. Parameters: (1) $m_a = 1.0$, $m_b = 0.0$; (2) $m_a = 0.9$, $m_b = 0.1$; (3) $m_a = 0.8$, $m_b = 0.2$; (4) $m_a = 0.7$, $m_b = 0.3$; (5) $m_a = 0.6$, $m_b = 0.4$; (6) $m_a = m_b = 0.5$. All subjects have the same $h = 0.3$, $\mu = 100$, $\theta = 1$, $n = 1$, $K^{\pm} = 1$ and refractory period $r = 1$. (b) Magnified plot at the origin of Figure 1(a). The solid lines are obtained by equation (1) (Poisson case) and the dashed lines by equation (18) (Gaussian case).

isolated netlets. The same curves in appropriate magnification are given in Figure 1(b). From these plots, we notice that, as expected, the different behavior of the neural activity at the origin for the Poisson and Gaussian approximations (Anninos & Elul, 1974) exists for all the above netlets with or without markers. We observe that for the case of two markers here, the Gaussian results are distinctly different from the Poisson ones, and the difference increases as the $(m_a - m_b)$ factor decreases. At the same time, we see that point A of the unstable steady-state (on the $x = y$ line), which exists here only in the Gaussian case, goes away from the origin. The curves in Figures 2(a) and 2(b) show the contribution of each marker to this behavior, for each one of the above six combinations of two markers.

The parameters of Figures 1 and 2 were varied to a large extent. We derived the behavior for nets with the following values of the other parameters, the same for each marker: $\mu^+ = \mu^- = 20, 50, 100, 200, 500$; $\theta = 1, 3, 5$; $h = 0, 0.1, 0.2, 0.3$; $|K^+| = |K^-| = 1$ and $A = 1000$ neurons. These plots are not shown here. The data for the entire variation of the parameters are in qualitative agreement. The general conclusion is that the numbers l_j and i_j $(j = 1, 2, \ldots, N)$ of EPSPs and IPSPs (which are the inputs to a given neuron for each marker) must be sufficiently large, justifying the replacement of the Poisson by a Gaussian distribution. Since their average values are $\bar{l}_j = a_n \mu_j^+ (1 - h_j) m_j$ and $\bar{i}_j = a_n \mu_j^- h_j m_j$ $(j = 1, 2, \ldots, N)$, it is obvious that the combination of all these parameters must be such as to give the appropriate average values (above 50 (Cox & Lewis, 1966, p. 21)) for each of the l_j and i_j. In Figures 3 and 4, we show networks of four subpopulations, i.e. four markers in each netlet: $m_a = 0.1$, $m_b = 0.2$, $m_c = 0.3$ and $m_d = 0.4$. For the sake of comparison, two different characteristic values for μ^+ were used: $\mu^+ = 20$, relatively small, and $\mu^+ = 200$, large enough to have considerably improved results for the Gaussian approach. The values of thresholds were selected such that we have all three classes, A, B and C, for the Poisson case (Harth *et al.*, 1970; Anninos *et al.*, 1970).

The curves in Figures 3(a) and 3(b) represent the total activity of each netlet for $\mu^+ = 20$ and 200, respectively. All three classes, A, B and C, are included here for the Poisson approximation, while only B or C classes appear in the corresponding Gaussian networks. In the upper right corner of Figure 3(b) a piece of the same plot at the origin for $\theta = 1$ is shown in magnification. For this value of θ, $\eta = 1$, (since $K^+ = 1$) and the Poisson network is of class A, even though the corresponding Gaussian net belongs to class B. The curves in Figure 3(b) with $\mu^+ = 200$ exhibit considerable agreement between the Poisson and Gaussian data and the crossing point A (see magnified plot) is very close to the origin, i.e. in a firing percentage about $a_n = 0.001$, which means one neuron out of 1000. However, in Figure 3(a) in which $\mu^+ = 20$ the differences between the two cases are large, requiring no magnification.

Figures 4(a) and 4(b) show the activities for each marker and the total network activity for the two nets of class B for the Poisson and also B for the Gaussian approximation, with the same parameters as in Figures 3(a) and 3(b), respectively. The contribution of each marker to the overall behavior of these networks can be seen in these plots. We observe that in Figure 4(a) $(\mu^+ = 20)$ each of the four differences (four lower groups of curves) contributes significantly to the difference in the total activity group (top group of curves). However, in Figure 4(b) $(\mu^+ = 200)$ all such differences are small, and for large a_n $(a_n > 0.4)$ they are extremely small. One can see that these differences are larger in the smaller markers (lower groups of curves).

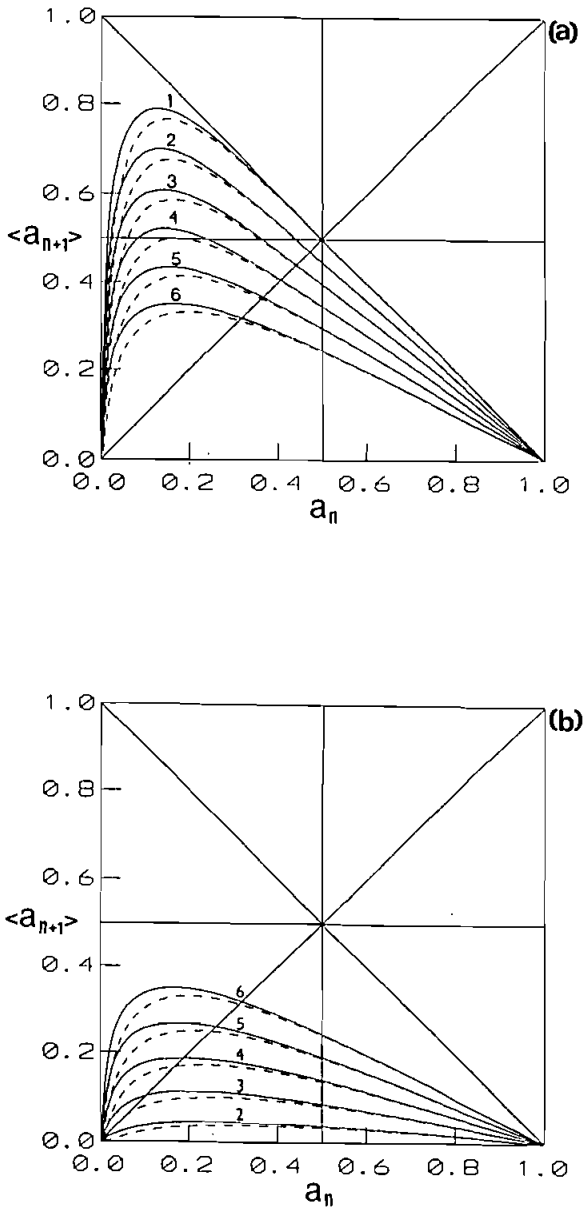

Figure 2. Contributions of the two subsystems a and b, (a) of marker a and (b) of marker b, on the total activity for each of the netlets of Figure 1. The numbers respectively indicate the netlets as referred to in Figure 1(a). The solid lines are used for the Poisson approximation while the dashed lines are for the Gaussian one.

On the basis of the same formalism, we also examine the time dependence of the neural activity for both cases, the Poisson and Gaussian one. Thus, we monitor the total activity of the net as a function of time, for several time units (synaptic delays), here $t = 15$. At time $t = 0$ the net is presented with some initial activity.

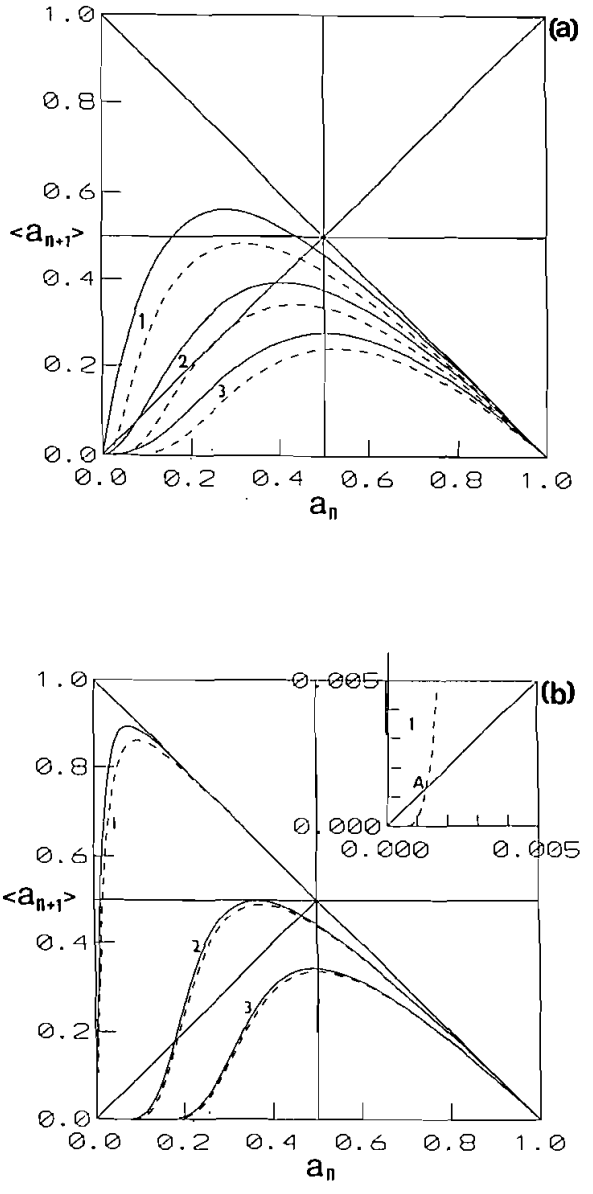

Figure 3. $< a_{n+1} >$ vs a_n for isolated netlets with four chemical markers, $m_a = 0.1$, $m_b = 0.2$, $m_c = 0.3$, $m_d = 0.4$, with $h = 0$, $K^+ = 1$ and refractory period $r = 1$. (a) Here all subnets have $\mu = 20$; for group 1, $\theta = 1$, $n = 1$; for group 2, $\theta = 2$, $n = 2$; for group 3, $\theta = 3$, $n = 3$. (b) Here all subnets have $\mu = 200$; for group 1, $\theta = 1$, $n = 1$; for group 2, $\theta = 15$, $n = 15$; for group 3, $\theta = 25$, $n = 25$. In the upper right corner, a magnified plot at the origin for $n = 1$ (group 1) is shown. The solid lines are obtained by equation (1) (Poisson case) and the dashed ones by equation (20) (Gaussian case).

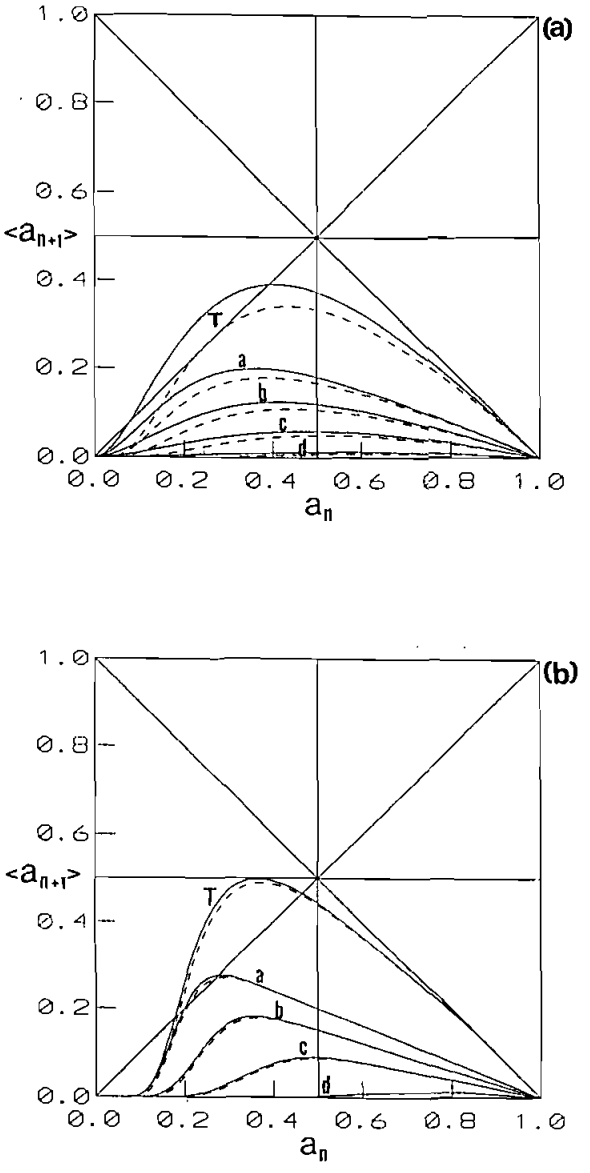

Figure 4. $< a_{n+1} >$ vs a_n for the netlets with four chemical markers and the same parameters as in Figure 3, for groups 2. (a) Here $\mu = 20$, $\theta = 2$, $n = 2$. (b) Here $\mu = 200$, $\theta = 15$, $n = 15$. The curves a–d represent the activities of each marker whereas T gives the total activity of the netlet. The solid lines are used for the Poisson case and the dashed ones for the Gaussian case.

Figures 5–7 show the results for the nets of Figure 3 with four markers. Group 1 of Figure 3(a) gives Figure 5(a) and Group 1 of Figure 3(b) gives Figure 5(b). Similarly, Group 2 produces Figure 6 and Group 3 produces Figure 7. We observe

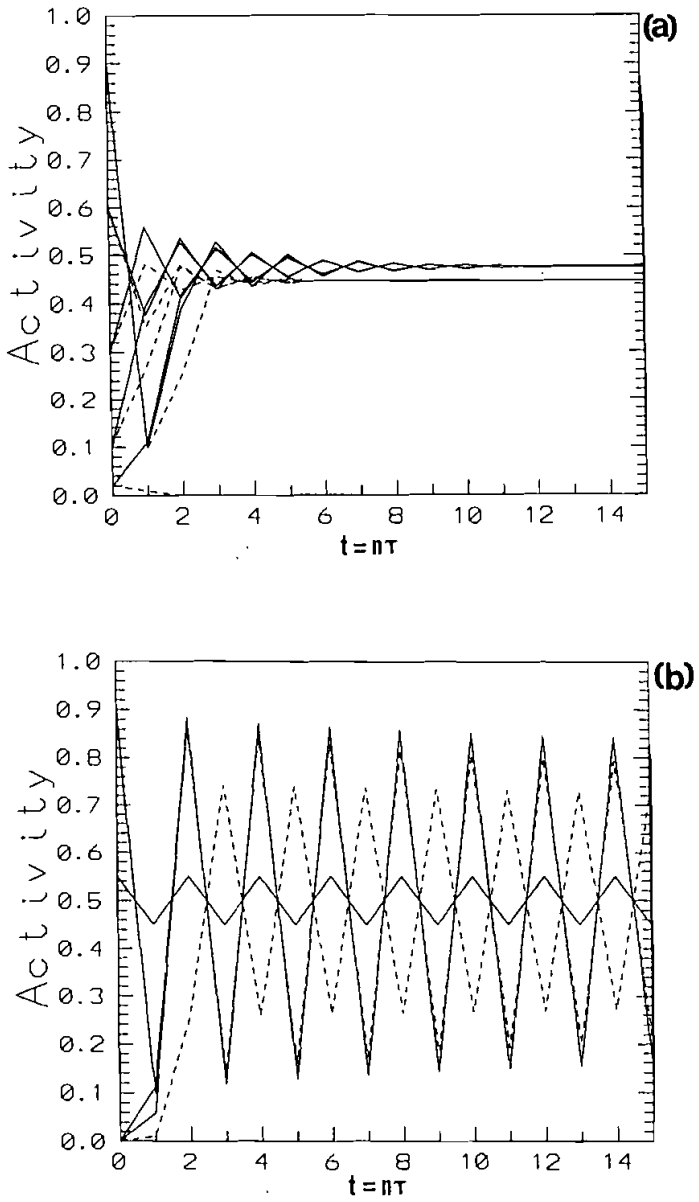

Figure 5. Time dependence of total activity a_n for the netlets of group 1 of Figure 3 with four markers *a*, *b*, *c* and *d*. (a) Initial activities: $a_0 = 0.02, 0.1, 0.3, 0.6$ and 0.9 for the parameters of Figure 3(a). (b) Initial activities: $a_0 = 0.001, 0.002, 0.55$ and 0.9 for the parameters of Figure 3(b). The solid lines are used for the Poisson approximation and the dashed ones for the Gaussian one.

that in Figure 5(a), after about $t = 10$ time delays, all initial activities collapse to the same value, $a = 0.48$ for the Poisson net, while for the Gaussian one most of them collapse more rapidly to a lower level of activity, $a = 0.45$. Only the smallest

of the five initial activities, $a_{01} = 0.02$, after a few time steps becomes eventually zero. Thus, the Poisson netlet behaves as an A class net while the Gaussian one behaves as a net of class B. In Figure 5(b), we observe similar behavior with respect to the distinction of classes in the two nets, but here the nets, due to the large value of μ^+ ($\mu^+ = 200$), exhibit strong oscillations about the same value, $a = 0.5$, in both cases. In Figures 6(a) and 6(b), we notice similar behavior for the two cases. Some initial activities, below the corresponding threshold of each case, after a few time steps become eventually zero, while the rest reach a stable steady state. All the networks here are of class B. The main difference however, is that in Figure 6(a) (with $\mu^+ = 20$) the attained level of activity ($a = 0.28$) in the Gaussian net is considerably below the level ($a = 0.39$) attained in the Poisson net, while in Figure 6(b) (with $\mu^+ = 200$) the attained levels are almost the same in both cases. Finally, in Figures 7(a) and 7(b) we notice that all curves lead to zero activity as these nets belong to class C.

4. Discussion

The principal question posed in the present study is whether differences in structure between various regions of the nervous system reflect, or perhaps even determine, distinct modes of function. Thus, the present study concentrated on analysis of the dynamic pattern of spike firing as represented in equation (20), which describes the relationship between the level of activity expressed in terms of the number of discharging neurons at a given period a_{n+1}, and the activity in the immediately preceding period a_n. Explicit solution for this equation has been derived in the present paper for the case where $P(a_n, m_j, \theta_j)$ is a normal variable. The corresponding solution for the Poisson case has been studied in detail in earlier work (Csermely, 1968; Harth *et al.*, 1969; Anninos *et al.*, 1970; Anninos & Kokkinidis, 1984). Comparison of these two sets of results shows that, given two nets with an identical proportion of excitatory and inhibitory synapses as well as firing threshold and the same markers, but differing in the functions $P(a_n, m_j, \theta_j)$, the resulting activity in the two cases is quite different, the Poisson net being capable of sustained activity under conditions in which activity in Gaussian nets would become quenched very rapidly (see Figures 1(b), 3(a) and 3(b)).

The question which must be dealt with at this point is that of the interpretation of the functions $P(a_n, m_j, \theta_j)$ in real nets in the CNS: do different $P(a_n, m_j, \theta_j)$ entail differences in structure of these nets, and if so, what are these differences?

To answer this question, we need to consider equation (20) in somewhat greater detail. This equation states that the number of firing neurons (as a percentage of the total neuron population) in a given cycle is determined by the number of neurons available for firing during that particular cycle. This is because $(1 - a_n)$ is the fraction of available neurons in the whole net, since those a_n neurons which fired in the preceding cycle are refractory during the current cycle. From the total number of neurons, only $(1 - a_n)m_j$ belong to marker j, and are available for firing. Equation (20) states, however, that in each marker only a fraction of the available population will fire, and that this fraction is determined by $P(a_n, m_j, \theta_j)$ for the jth marker. According to whether a Gaussian or Poisson probability function is selected, $P(a_n, m_j, \theta_j)$ will either be a Gaussian or Poisson variable determined by a_n. Specifically, the value of $P(a_n, m_j, \theta_j)$ in successive cycles would be distributed according to either normal or Poisson distribution, with the independent variable being the number of neurons firing in the preceding cycle a_n.

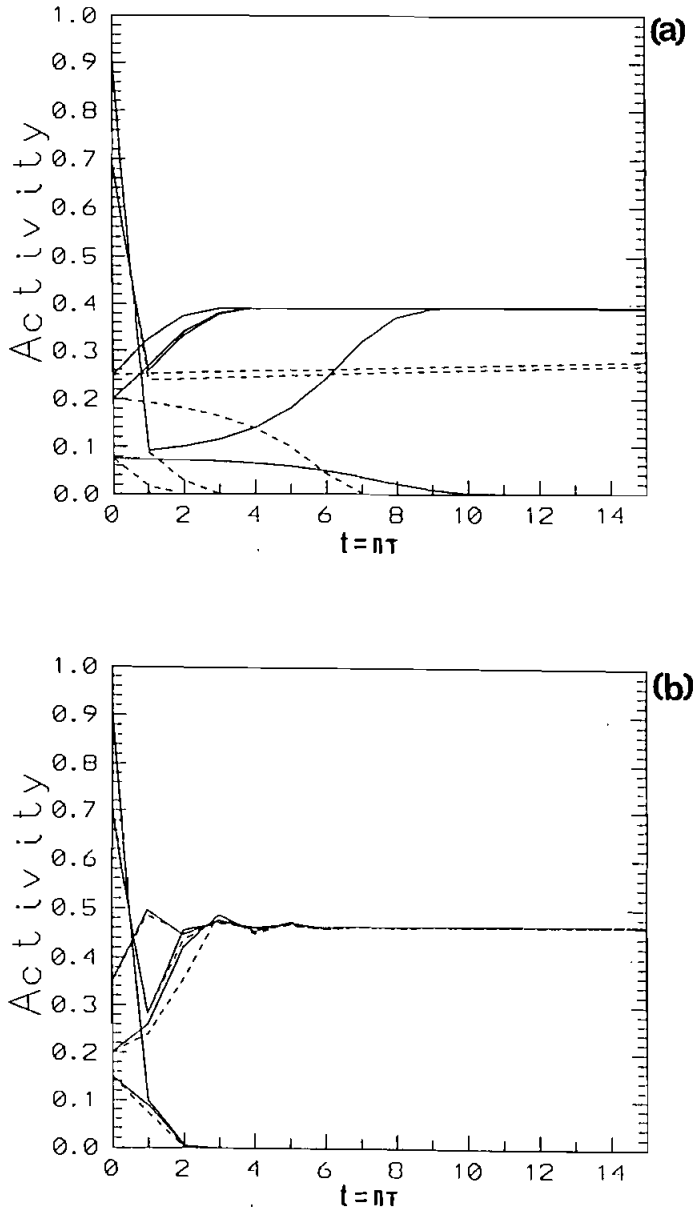

Figure 6. Time dependence of total activity a_n for the netlets of group 2 of Figure 3 with four markers *a*, *b*, *c* and *d*. (a) Initial activities: $a_0 = 0.075$, 0.2, 0.25, 0.7 and 0.9 for the parameters of Figure 3(a). (b) Initial activities: $a_0 = 0.15$, 0.2, 0.35, 0.7 and 0.9 for the parameters of Figure 3(b). The solid lines are used for the Poisson approximation and the dashed ones for the Gaussian one.

It is appropriate to enquire how this functional dependence can be satisfied in 'real' neuronal nets, i.e. in nets where the pattern of interneuronal connections is unalterable. One way to answer this question is to investigate if the number

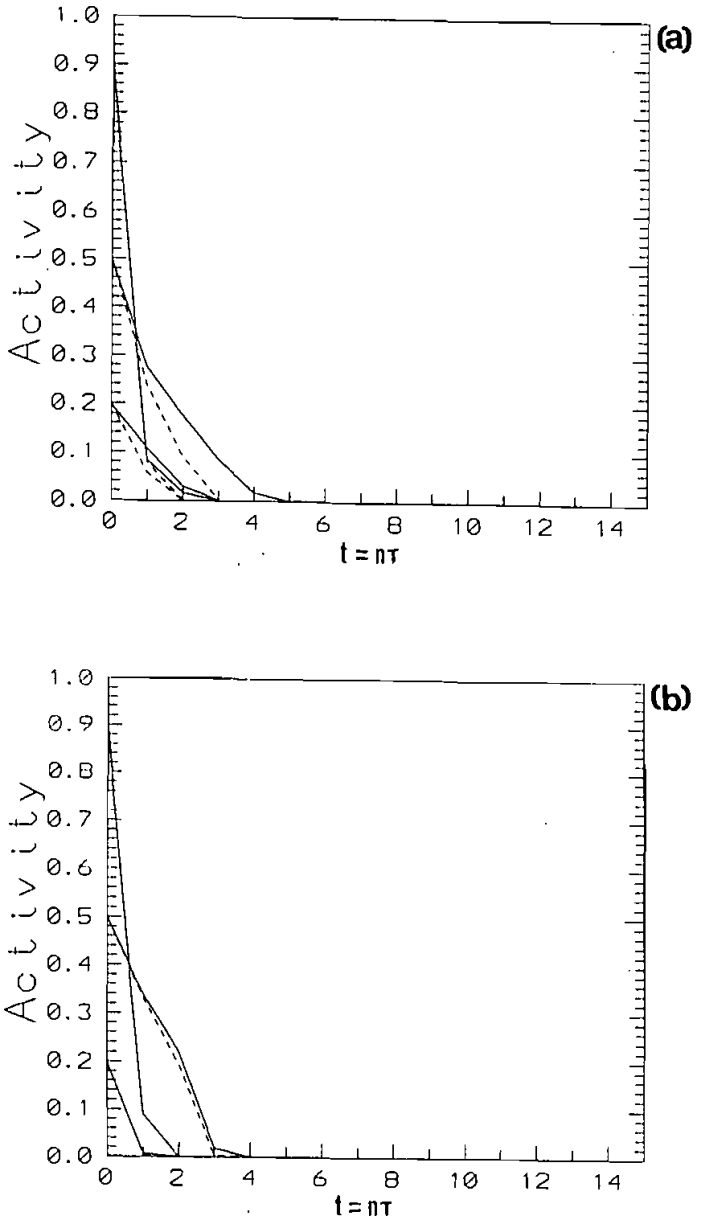

Figure 7. Time dependence of total activity a_n for the netlets of group 3 of Figure 3 with four markers *a*, *b*, *c* and *d*. (a) Initial activities: $a_0 = 0.2$, 0.5 and 0.9 for the parameters of Figure 3(a). (b) Initial activities: $a_0 = 0.2$, 0.5 and 0.9 for the parameters of Figure 3(b). The solid lines are used for the Poisson approximation and the dashed ones for the Gaussian one.

of synaptic connections received by each cell would vary as a Gaussian or, alternatively, a Poisson variable. Based on the assumption that synaptic potentials sum algebraically—an assumption which is widely accepted in regard to the

analysis of physiological data (see, however, Elul & Adey, 1966 for further discussion)—it is clear that different cells in the net would have a different probability of discharging following the discharge of, say, 10% of the cells in the immediately preceding cycle. Moreover, on the assumption of algebraic summation of synaptic inputs, the firing probabilities of these cells, being directly related to the number of afferent connections, will be distributed following a Poisson or Gaussian probability distribution, respectively. In this way, equation (20) will be satisfied in nerve nets in which the number of connections received by each cell (and in a closed system—also originating in each cell) represents a Poisson or, alternatively, a Gaussian variable. Our results may therefore be restated as follows: a neuronal net where the number of connections received by each neuron is distributed according to a Poisson function will exhibit sustained activity. On the other hand, a net in which the number of connections reaching each particular nerve cell varies according to a normal distribution will not be capable of sustained activity.

These results are of significant interest in pointing to a hitherto unconsidered parameter, which may be worthy of examination in histological material: the probability distribution of the number of synapses received by individual cells in a given nucleus or region of the brain. Although there are a number of studies in the literature dealing with quantitative aspects of synapse populations, the variance and the mean of counts in individual neurons have not been documented in most of these studies, and the probability function of distribution of these connections has not been investigated.

Notwithstanding the absence of specific information on the probability distribution of the numbers of synaptic inputs to individual neurons in different brain structures, we may proceed in our investigation of the present results in a more general fashion, giving certain well-known properties of the normal distribution. It is important to recall in this context that, for a large number of events (i.e. in our model, a large number of interconnections), the Poisson distribution converges toward the normal distribution (cf., for example, Feller, 1957, pp. 176–178; Cox & Lewis, 1966, Chapter 1). Thus Poisson neuronal nets may be viewed as approximately Gaussian whenever the number of synaptic connections is relatively large. Insofar as the normal distribution is the limiting distribution for a great many experimental distributions when the number of elements becomes large, it is also likely that, in general, most systems with large numbers of synaptic connections per never cell would tend toward the Gaussian case discussed in the present study. For these reasons, it appears that the conclusions reached here regarding nets characterized by Gaussian probability law may be applicable within the limitations of the basic assumptions of the model, and with only minor modification, to most real neuronal centers for which there is histological evidence of rich systems of interconnections. Indeed, these results would equally apply also to nerve nets with Poisson distribution of interconnections, provided only that the average number of connections (the Poisson parameters λ) is above 50 (cf., for example, Cox & Lewis, 1966, p. 21). Thus, our results may be further generalized to suggest that the average number of interneuronal connections in a given CNS structure may be the significant parameter in determining spontaneous activity: all structures having large numbers of interconnections per nerve cell would be unlikely to exhibit intrinsic sustained activity. Such spontaneous activity appears from our results to be more likely to originate in neuronal nets with small average number of synapses per neuron.

Acknowledgements

We would like to thank Dr B. Kargas for useful discussions and for his help in preparing the manuscript. This project was supported by grant no. E5/3667/1989 by the Ministry of Education (Athens).

References

Anninos, P.A. & Elul, R. (1974) Effect of structure on function in model nerve nets. *Biophysics Journal*, **14**, 8–19.

Anninos, P.A. & Kokkinidis, M. (1984) A neural net model for multiple memory domains. *Journal of Theoretical Biology*, **109**, 95–110.

Anninos, P.A., Beek, B., Csermely, T.J., Harth, E.M. & Pertile, G. (1970) Dynamics of neural structures. *Journal of Theoretical Biology*, **26**, 121–148.

Cox, D.R. & Lewis, A.W. (1966) *The Statistical Analysis of Series of Events*. London: Methuen.

Csermely, T.J. (1968) Doctoral Dissertation, Syracuse University, Syracuse, NY.

Elul, R. & Adey, W.R. (1966) Instability of firing threshold and 'remote' activation in cortical neurones. *Nature (London)*, **212**, 1424–1425.

Feller, W. (1957) *An Introduction to Probability Theory and its Applications*. New York: Wiley.

Harth, E.M., Csermely, T.J., Beek, B. & Lindsay, R.P. (1969) Aerospace Medical Laboratories AMRL-TR-68–189, Aerospace Medical Division, Air Force Systems Command, Wright-Patterson Air Force Base, Ohio.

Harth, E.M., Csermely, T.J., Beek, B. & Lindsay, R.P. (1970) Brain functions and neural dynamics. *Journal of Theoretical Biology*, **26**, 93–120.

Prestige, M.C & Willshaw, D.J. (1975) On a role for competition in the formation of patterned neural connections. *Proceedings of the Royal Society, London*, B, **190**, 77–98.

Sperry, R.W. (1943) Visumotor co-ordination in the newt (*Triturus viridecens*) after regeneration of the optic nerve. *Journal of Comparative Neurology*, **79**, 33–55.

Sperry, R.W. (1963) Chemoaffinity in the orderly growth of the nerve fiber patterns and connections. *Proceedings of the National Academy of Sciences, USA*, **50**, 703–709.